Egypt. J. Chem. **Vol. 61**, No.1, pp. 101 - 119 (2018)

Tamarixaphylla Biomass as an Efficient Adsorbent for Removal of Pb(II) Ions from Aqueous Solution: Kinetic and Applicability for Different Isotherm Models

Magdy D. Madbouly[1] and A. Al-Anwar[2]
[1] *National Centre for Social and Criminal Research, Cairo, Egypt.*
[2]*Assuit Laboratory, Medico-legal Department, Ministry of Justice, Assuit, Egypt.*

TAMARIXAPHYLLA biomass (TAB) is a low cost adsorbent that has been used for the removal of Pb(II) ions from an aqueous solution. It was characterized by Fourier Transform Infrared Spectroscopy (FT-IR) and Scanning Electron Microscopy (SEM) to support the adsorption of Pb(II) ions. The ability of TAB to adsorb Pb(II) ions was investigated by using batch adsorption procedure. The effects of various parameters such as solution pH, adsorbent concentration, contact time and initial Pb(II) ions concentration were examined. The adsorbent data were analyzed using two, three, four and five parameter models at 30^{o}C by using nonlinear regression analysis.Various kinetic models including the Pseudo-first-order, Pseudo-second-order, Elovich, Intra-particle diffusion and Bangham models have been applied to the experimental data to predict the adsorption mechanism. It was found that pseudo-second-order rate was better obeyed than pseudo-first-order reaction supporting that chemisorption process was involved. The examination of error analysis methods showed that the Langmuir model provide the best fit for experimental data than other isotherms. The obtained results show that TAB can be used as an effective and a natural low-cost adsorbent for the removal of Pb(II) ions from aqueous solutions.

Keywords: Tamarixaphylla, Pb (II) ions, adsorption, aqueous solution, Isotherm models, adsorption kinetics.

Introduction

Heavy metal pollution is one of the world's most important environmental issues since heavy metals show high toxicity due to their solubility in water and easily accumulation in living organisms. Heavy metal contamination in wastewater is generated from various industrial processes such as mining, iron and steel, painting, and battery manufacturing [1].

Lead is a soft, malleable, ductile and dense metal. Due to its corrosion resistant characteristics, Pb has been historically used in plumbing. The other major use of Pb is in lead-acid batteries manufacturing and formation of lead alloys. However, as, lead is toxic in nature. The high exposure to Pb can increase the risk of kidney failure, disruption of central nervous system, brain damage and even death [2]. There are different methods to treat the wastewater; the treatment methods are based on the level of the waste and the cost of treatment [3]. Conventional methods for the removal of the heavy metal ions from wastewater include chemical precipitation, electro flotation, ion exchange, reverse osmosis and adsorption onto activated carbon. These methods have been found to be limited, since they often involve high capital and operational costs, incomplete removal [4] and may be associated with the generation of secondary waste which is again to be treated or to be safely disposed off [5].

Adsorption provides one of the most effective methods for removing heavy metal ions from aqueous solutions[6]. Activated carbon is the most widely used adsorbent for this purpose because of its extended surface area, microporous structure, high adsorption capacity and high degree of surface reactivity. However, commercially activated carbons are very expensive [7]. This led to search for cheaper adsorbent for heavy metal removal. The agricultural wastes [8] were considered as low-cost since they 1) require little processing and

*Corresponding author e-mail: magdydiab@su.edu.sa
DOI: 10.21608/ejchem.2018.1636.1138

2) are abundant in nature. Commonly, it concerns vegetal materials, and then the term of biosorption is used to designate the fixation of contaminants onto biomaterials. Recently, numerous low-cost alternative adsorbents have been examined for the removal of Pb(II) ions from wastewater [9-14]. The abundant and availability of TAB residues makes them a good candidate for incorporation as bio-adsorbent of heavy metals from wastewater.

The aim of the present work is to explore the possibility of utilizing TAB for the adsorption of Pb (II) ions from aqueous solutions. The effect of such factors as pH, adsorbent dose, adsorbate concentration, contact time and initial concentration was investigated. Experimental equilibrium data were fitted to the Freundlich, Langmuir, Dubinin–Radushkevich, Halsey and Temkin (two parameter models), Redlich–Peterson, Sips, Khan, Hill, Radke-Prausnitz, Langmuir-Freundlich and Toth (three parameter models), Fritz–Schlunder and Baudu (four parameter models) and Fritz–Schlunder (five parameter model) at 30 °C by using non-linear regression analysis. Error analysis was carried out to test the adequacy and the accuracy of the isotherm models. The kinetics of Pb(II) ions adsorption on the adsorbent was analyzed by fitting various kinetic models.

Experimental

Materials

Bioadsorbent

Tamarixaphylla plant is widely spread in West Desert in Egypt and was obtained from Matrouh Desert (Egypt). The roots were separated from the stems and leaves, washed with distilled water several times until the filtrate was colourless to remove the surface adhered particles and water soluble particles. The roots were dried in an electric oven at 105 °C for 3 h, then finally ground using a mixer, and sieved to pass through a 50 - 150 µm. The roots were chosen because the previous studies indicated that the cellulose content in roots is usually higher than in leaves and stems [8].

Reagents

Lead acetate, EDTA, sodium hydroxide and nitric acid were all used as laboratory grade chemicals(Merck, Darmstadat, Germany).

Characterization of adsorbent

The Fourier Transform Infrared Spectrometer (FT-IR) analysis was used to identify the different functional groups present in TAB and Pb (II) ions loaded TAB. The IR spectra were recorded on a Perkin-Elmer Spectrum 1000 spectrophotometer over 4000-400 cm^{-1} using KBr disk technique.

Scanning Electron Microscope (SEM), JEOL JSM 840, was used to obtain the surface morphology of TAB residues before and after Pb adsorption.

Methods

Adsorption studies

A known volume (100 mL) of a Pb(II) ions solution with a concentration in the range 100–1000 mg L^{-1} was placed in a 125 ml Erlenmeyer flask. An accurately weighed sample of TAB adsorbent (0.05 g) with a particle size in the range 50–150µm was then added to the solution. A series of such flasks were prepared, the pH values of the contents adjusted by the addition of 0.1 M HNO_3 or 0.1 M NaOH and then shaken at a constant speed of 150 rpm in a shaking water bath at 30°C for two hours. At the end of the agitation time, the metal ion solutions were separated by filtration. Blank experiments were carried out simultaneously without the addition of the TAB adsorbent. The extent of metal ion adsorption onto adsorbent was calculated mathematically by measuring the metal ion concentration before and after the adsorption through direct titration against the standard EDTA solution. The amount of Pb(II) ions adsorbed on TAB at equilibrium, q_e (mg/g) and percent removal of lead were calculated according to the following relationships:

$$q_e = \frac{(C_o - C_e).V(l)}{W} \quad (1)$$

$$\text{Percent Removal} = \frac{C_o - C_e}{C_o} x100\% \quad (2)$$

where C_o and C_e are the initial and final concentrations of Pb (II) ions, mgL^{-1}, V(l) is the volume of adsorbate, W is the weight of TAB adsorbent (g). All experiments were carried out in duplicate and the mean values of q_e were reported.

Error Analysis

In the single-component isotherm studies, the optimization procedure requires an error function to be defined to evaluate the fit of the isotherm to the experimental equilibrium data. The common error functions for determining the optimum

isotherm parameters were, sum of absolute errors (EABS), Marquardt's percent standard deviation (MPSD), average percentage error (APE) and average relative error (ARE)[15]. In the present study, all error functions were used to determine the best fit in isotherm model as:

The Sum of Absolute Error (EABS)

$$EABS = \sum_{i=1}^{n} \left| (q_e)_{\text{exp.}} - (q_e)_{calc.} \right|_i \quad (3)$$

Marquardt's Percent Standard Deviation MPSD

$$MPSD = \left(100 \sqrt{\frac{1}{n-p} \sum_{i=1}^{n} \left[\frac{((q_e)_{\text{exp.}} - (q_e)_{calc.})}{(q_e)_{\text{exp.}}} \right]^2} \right) \quad (4)$$

Average Percentage Error (APE)

$$APE\% = \frac{\sum_{i=1}^{N} \left| [((q_e)_{\text{exp.}} - (q_e)_{calc.}) / q_{\text{exp.}}] \right|}{N} x100 \quad (5)$$

$$ARE = \sum_{i=1}^{n} \left| \frac{(q_e)_{\text{exp.}} - (q_e)_{calc.}}{(q_e)_{\text{exp.}}} \right|_i \quad (6)$$

Results and Discussion

Characterization of adsorbent

FTIR Studies

The FT-IR spectra for native and Pb loaded TABwere recorded (Fig. 1 above and down) to identify the different functional groups of TAB responsible for lead removal. The broad band positioned around 3389 $cm^{-1}$was assigned the stretching vibration of hydroxyl groups. The high content of water in the TAB and numerous hydroxyl groups in the polysaccharide structure of the plant cell walls explained the presence of this band. The appearance of a band at 1737 cm^{-1}in the Pb loaded TAB can be assigned to the carboxylate ion ($–COO^-$). At pH greater than 4.0, the carboxylic acid group is converted to the carboxylate ion and Pb (II) ions are adsorbed. The involvement of carboxylic acid groups in the adsorption process explains the effect of pH on the adsorption process. At pH 2.0, majority of the carboxylate ions are converted to carboxylic acid groups (–COOH) and hence the adsorption efficiency decreases. However, the broadening of the peak (Fig. 1above) decreases (Fig. 1 down) indicating that the hydrogen bonding of the hydroxyl groups decreases after Pb loading. All these observations indicate the involvement of functional groups like carboxylic acid in the biosorption process.

The adsorption bands at 3389, 2931, 1736, 1631, 1460, 1371, 1238, 1038and 605 cm^{-1}(Fig. 1a) had shifted, respectively, to 3420, 2923, 1737, 1631, 1462, 1367, 1241, 1038and 573 cm^{-1} due to Pb (II) ions absorption (Fig. 1b). These shifts might be attributed to ion exchange associated with carboxylate and hydyroxylate anions, suggesting that acidic, carboxyl and hydroxyl groups, were predominant contributors in metal

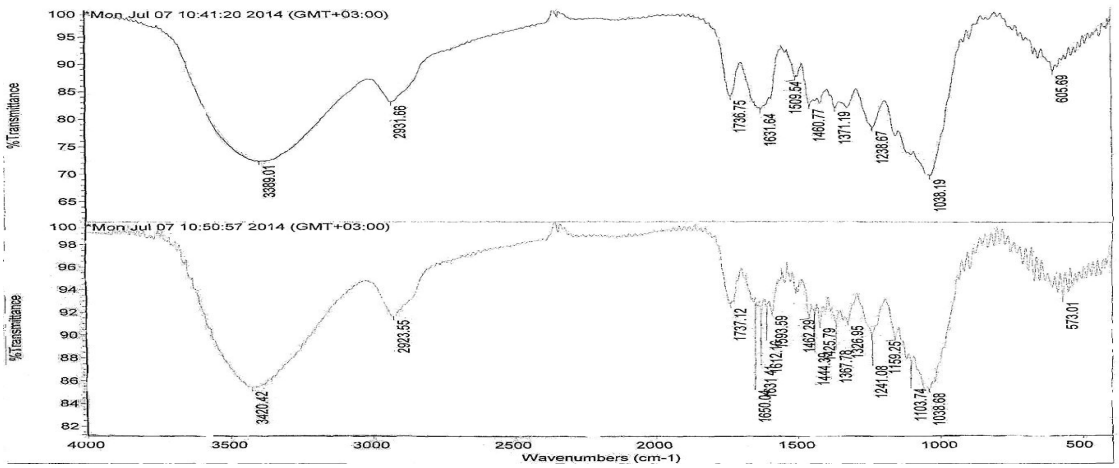

Fig. 1. FT-IR of TAB (above) and Pb (II) ions-loaded TAB (down)

ion uptake [16]. To investigate the adsorption process further, the TAB and Pb (II) ions loaded TAB were observed under the scanning electron microscope.

SEM studies

The SEM images of the TAB and Pb loaded TAB are shown in Fig. 2. SEM image of the powdered TAB (Fig. 2a) shows a regular symmetry with hollow tubular structures before adsorption. After Pb adsorption, the tubes appear to be prominently swollen as Pb enters the pores of the TAB(Fig. 2b). This observation indicates that Pb is adsorbed to the functional groups of the TAB structure.

Factors Affecting Adsorption of Pb(II) Ions onto TAB

The biosorption process of heavy metals is influenced by several factors, such as pH, adsorbent dose, contact time and adsorbate concentration. The effects of these parameters were investigated in this section.

Effect of pH

The pH of the aqueous solution is an important controlling parameter in the adsorption process [17]. In the present work, adsorption of Pb (II) ions ontoTAB adsorbent was studied over the pH range of 2- 4.5 for a constant adsorbent dose and constant concentration of adsorbate at 30 °C. As the acidity of the adsorption medium decreased, the extent of adsorption capacity, q_e decreased (Fig. 3). At high acidity, the TAB particle surface will be completely covered with H_3O^+ ions and Pb (II) ions can hardly compete with them for adsorption sites. With the increase in pH, the competing effect of hydronium ion decreases and the positively charged Pb (II) ions adsorb on the free binding sites of the adsorbents. This is a common observation for all cases of adsorption of metal cations on the solid surface in media of different acidity and basicity [18]. It is also significant that the active sites on the TAB are weakly acidic in nature and with increase in pH, they are gradually deprotonated making available more and more sites for metal ion uptake [19]. At pH value more than 4.5, the adsorption studied

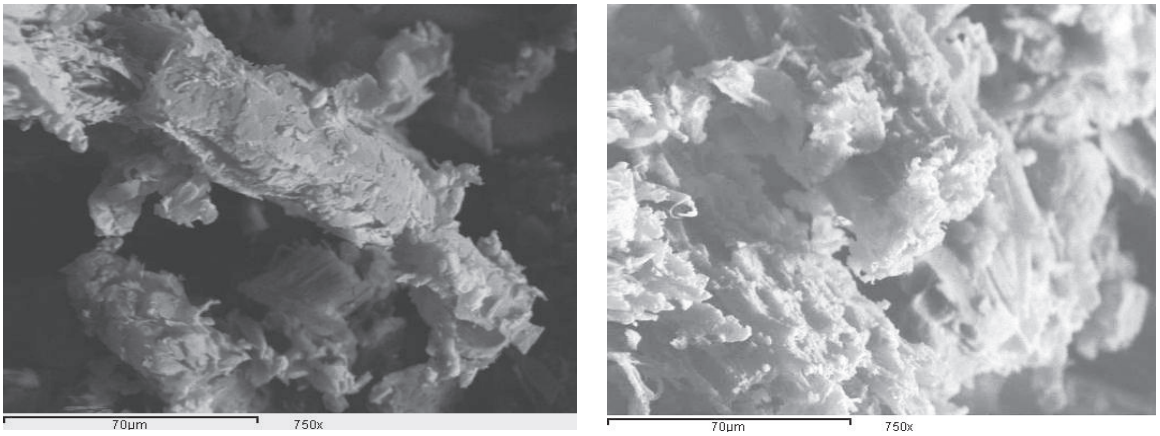

Fig. 2. SEM of TAB (above) and Pb(II) ions-loaded TAB (down).

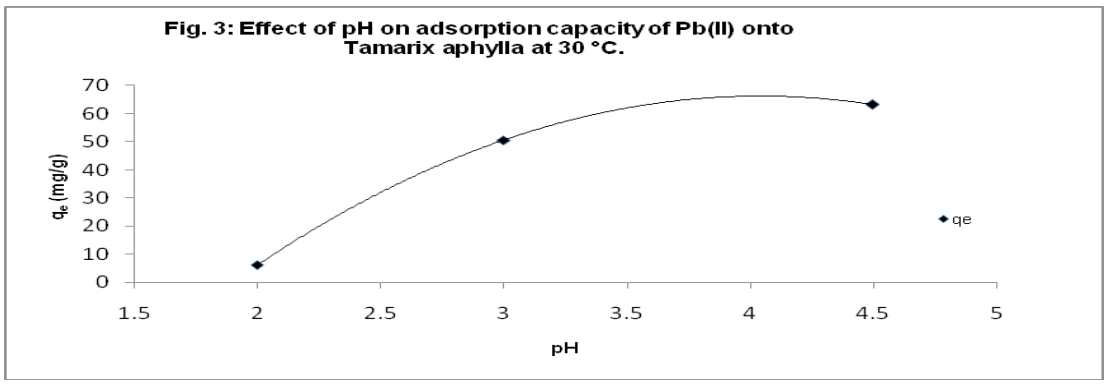

could not be carried out because metal ion will precipitate as lead hydroxide in this range [20].

Effect of Adsorbent Concentration (Adsorbent Dose)

The effect of adsorbent dose on both the adsorption capacity and the percentage removal of Pb (II) ions onto TAB were studied at pH 4 employing adsorbent doses within the range 0.3–5 g/land at a fixed initial metal ion concentration of 300 mg L^{-1} as shown in Fig.4. It is clear from this figure that the percent removal of Pb (II) ions increases from 12.2 to 88.2 % by increasing the concentration of adsorbent from 0.1 to 5 g/l. The increase in percent removal of Pb (II) ions with increasing adsorbent concentration could be attributed to the greater availability of the exchangeable sites of the adsorbent. On the other hand, the adsorption capacity (q_e), or the amount of Pb (II) ions adsorbed per unit mass of adsorbent (mg/g), decreases by increasing the concentration of adsorbent (Fig. 4). The decrease in adsorption capacity with increasing the adsorbent concentration is mainly due to overlapping of the adsorption sites as a result of overcrowding of the adsorbent particles and is also due to the competition among Pb(II) ions for the surface sites [21].

Effect of Contact Time

Figure 5 shows the effect of agitation time at two different adsorbate concentrations (324 and 542 mg L^{-1}) on the adsorption capacity of TAB towards Pb (II) ions. It will be seen that the adsorption capacity increased with increasing agitation time and initial concentration of the adsorbate, remaining virtually constant after equilibrium had been attained. The time necessary to achieve equilibrium increased with increasing adsorbate concentration, being 30and 60 min for adsorbate concentrations of 324 and 542 mg L^{-1}, respectively. This contact time, which is one of the parameters for economical wastewater treatment plant operations, is quite small.

Kinetics of Adsorption: In order to examine the controlling mechanism of biosorption process such as mass transfer and chemical reaction, kinetic models were used to test experimental data. Many applications, such as wastewater treatment and metal ions removal need a rapid biosorption rate and short contact time. The kinetic models (pseudo-first-order, pseudo-second-order, intraparticle diffusion and Bangham and Elovich models) were used to investigate the adsorption process of Pb(II) ions on TAB.

The pseudo-first-order equation [22] is:

$$\frac{dq_t}{dt} = k_1(q_e - q_t) \quad (7)$$

Where q_t is the amount of adsorbate adsorbed at time t (mg/g), q_e is the adsorption capacity at equilibrium (mg/g), k is the pseudo-first-order rate constant (min^{-1}), and t is the contact time (min). The integration of Eq. (7) with the initial

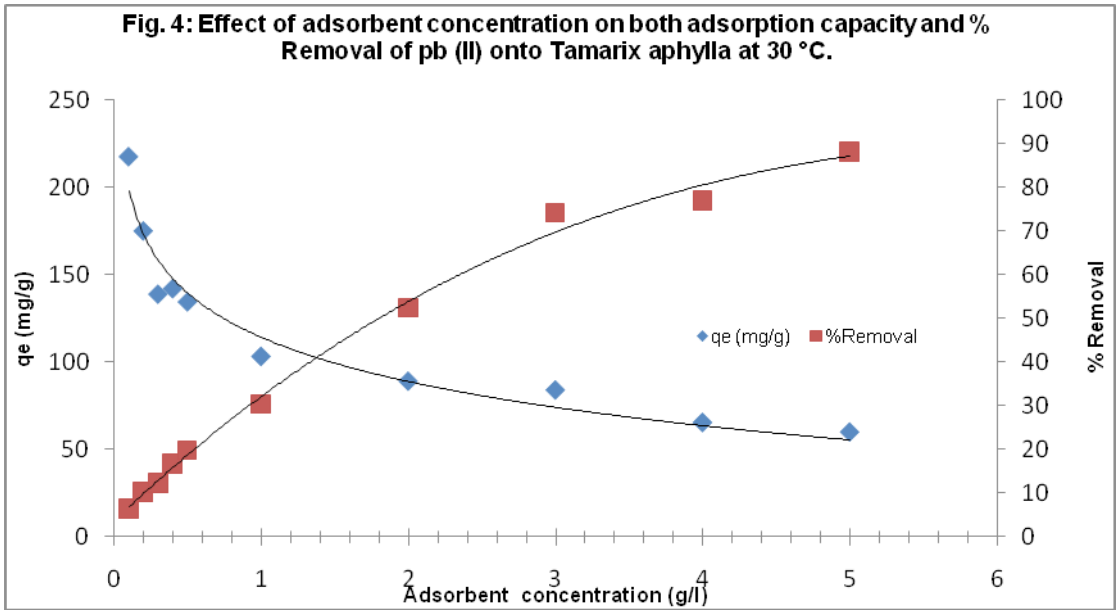

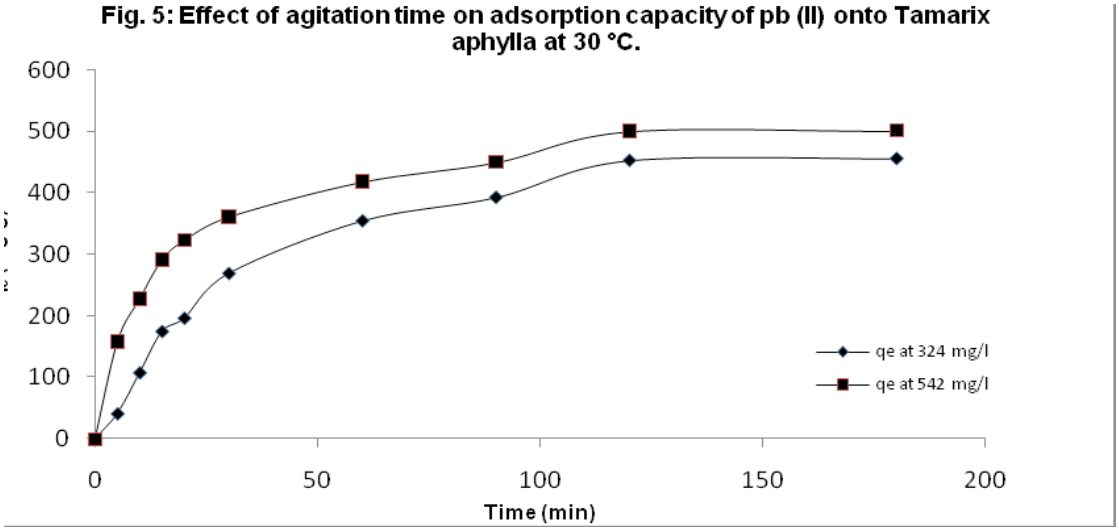

condition, $q_t = 0$ at $t = 0$, the following equation is obtained:

$$\log(q_e - q_t) = \log q_e - \frac{k.t}{2.303} \quad (8)$$

A first-order kinetic process is usually considered physical biosorption and the whole process is diffusion controlled.

In order to obtain the rate constants, the straight line plot of log (q_e-q_t) against t for Pb (II) ions onto TAB have been tested. The intercept of this plot should give log q_e. However, if the intercept does not equal to q_e, the reaction is not likely to be first order even if this plot has high correlation coefficient (R^2) with the experimental data [23]. For the data obtained in the present study, the plots of log (q_e–q_t) versus t as required by Eq. 8 for the adsorption of Pb (II) ions at initial concentrations of 324mg L^{-1} and 542 mg L^{-1} by TAB (figure not shown) gave correlation coefficients, R^2, which had low values. This indicates that the adsorption of Pb (II) ions onto TAB is not acceptable for this model.

The pseudo-second-order model [23] is represented as:

$$\frac{dq_t}{dt} = k_2(q_e - q_t)^2 \quad (9)$$

where k_2 is the pseudo-second-order rate constant (g /mg.min). Integrating Eq. (9) with the initial condition, $q_t = 0$ at $t = 0$, the following equation is obtained:

$$\frac{t}{q_t} = \frac{1}{(k_2.q_e^{\,2})} + \frac{t}{q_{e_t}} \quad (10)$$

where k_2 is the pseudo–second-order adsorption rate constant.

Equation 10 predicts that if the system follows pseudo–second-order kinetics, the plot of t/q_e versus t should be linear. Plotting the experimental data obtained for the adsorption of Pb (II) ions at initial concentrations of 324mg L-1 and 542 mg L^{-1} onto TAB according to the relationship given in Eq. (10) gave linear plots (Fig. 6).

The correlation coefficient values (R^2) were 0.972 and 0.998 for the initial concentrations of 324 mg L^{-1} and 542 mg L^{-1}, respectively obtained from the pseudo-second-order model making them larger than those of the pseudo-first-order model (or the other applied models). The results obtained from the pseudo-second-order model were the best for describing the kinetics of Pb (II) ions onto TAB as shown in Fig. 6 and listed in Table 1. The first-order and pseudo–second-order models cannot identify the diffusion mechanism and the kinetic results were then subjected to analyze by the intra-particle diffusion model.

The intra-particle diffusion model [24] can be expressed by the following equation:

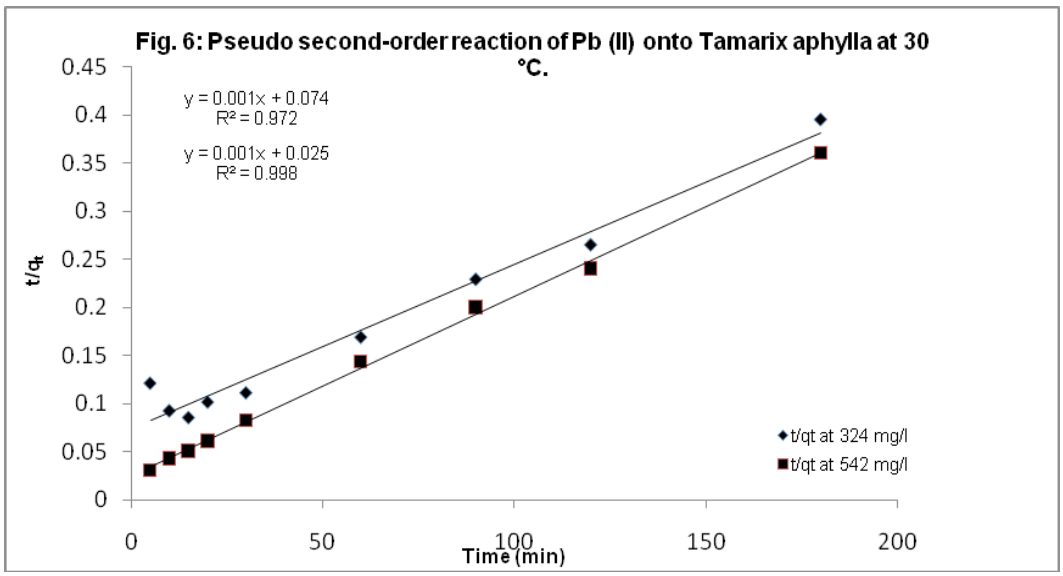

TABLE 1. Kinetic parameters for adsorption of Pb(II) onto TAM at 30 °C

Models	Parameters	Values (324 mg/l)	Values (542 mg/l)
Pseudo-first order	K_1	----------	----------
	R^2	----------	----------
Pseudo-second order	K_1	3.884E-05	0.0001399
	q_e (exp)	452.03492	499.45117
	q_e (Calc.)	588.23529	526.31579
	R^2	0.9726	0.9981
Bangham's Equation	K_o	6.93063	21.05585
	α	0.6905	0.3400
	R^2	0.9121	0.9414
Intra-Particle Diffusion	Kp	38.072	24.892
	C	43.957	218.08
	R^2	0.9569	0.9841
Elovich Equation	α	33.032356	113.50012
	β	0.0080658	0.0102069
	R^2	0.9906	0.9853

$$q_t = k_P . t^{\frac{1}{2}} + C \quad (11)$$

Where k_p is the intra-particle diffusion rate constant (mg. $g^{-1}.min^{-1/2}$) and q_t is the amount of solute adsorbed per unit mass of the adsorbent. The data of solid phase metal concentration against time t at the initial concentrations of 324.3mg/l and 542.4 mg/l of Pb (II) ions were further processed for testing the rate of diffusion in the adsorption process.

The rate parameter for intra-particle diffusion, k_p for the Pb (II) ions on TAB is measured according to Eq. 11. The plots of $q_t$versus $t^{1/2}$ for the Pb (II) ions concentrations of 324mg $L^{-1}$and 542 mg L^{-1} of is shown in Fig. 7. Different

previous studies indicated that the plots of q_t versus $t^{1/2}$ were multi-linear two or more steps govern the adsorption process [25-27]. The plot is curved at the initial portion followed by linear portion and plateau. The initial curved portion is attributed to the bulk diffusion and the linear portion is due to the intra-particle diffusion, while the plateau is corresponding to equilibrium. The deviation of straight lines from the origin (Fig. 8) may be due to the difference between the rate of mass transfer in the initial and final stages of adsorption. Further, such deviation of straight line from the origin indicates that the pore diffusion is not the rate-controlling step [28]. The values of k_p (mg. $g^{-1}.min^{-1}$) obtained from the slope of the straight line (Fig.8) are listed in Table 1. The values of R^2 for the initial concentrations of 324 mg $L^{-1}$and 542 mg L^{-1} are listed also in Table 1. The value of intercept, C (Table 1) give an idea about the boundary layer thickness, i.e., the larger the intercept, is the greater the boundary layer effect [29]. This value indicates that the adsorption of Pb(II) ions onto TABis acceptable for intra-particle diffusion mechanism.

Bangham's equation [30] was employed for applicability of adsorption of Pb (II) ions onto ATB, whether the adsorption process is diffusion controlled as follows:

$$\log\log\left(\frac{C_o}{C_o - q.m}\right) = \log\left(\frac{k_o m}{2.303V}\right) + \alpha \log t \quad (12)$$

where C_o is the initial concentration of adsorbate (mg L^{-1}), V is the volume of metal ion(ml), m is weight of adsorbent used per liter of solution (gL^{-1}), q is the amount of adsorbate retained at time t (mg/g), $1 > \alpha$) and k_0 are constants.

If the experimental data are compatible with Bangham's equation, the biosorption kinetics is limited to the pore diffusion.

The double logarithmic plot, according to Eq. 12 yields satisfactory linear curves for the adsorption of Pb (II) ions by TAB (Fig. 9). The correlation coefficient values, R^2 values were 0.9121 and 0.9414 for the initial concentrations of 324 and 542 mg L^{-1}, respectively. This indicates that the adsorption of Pb (II) ions onto TAB is acceptable for this model.

The Elovich model equation [31]is generally expressed as:

$$\frac{dq_t}{dt} = \alpha \exp(-\beta . q_t) \quad (13)$$

Where α is the initial adsorption rate (mg/g. min) and β is the adsorption constant (g/mg) during the experiment. To simplify the Elovich equa ned αβ >>1ε ons q = 0 at t me:

$$q_t = \frac{1}{\beta}\ln(\alpha\beta) + \frac{1}{\beta}\ln(t) \quad (14)$$

If Pb(II) ions adsorption onto TAB fits the Elovih model, a plot of q_e versus ln t should yield a linear relationship with a slope of $1/\beta$ and an intercept of $1/\beta \ln(\beta$). Figure 10 shows a plot of linearization form of Elovich model at the Pb (II) ions concentrations of 324mg L^{-1} and 542 mg L^{-1}. The slope and intercept of the plots of q_t versus ln(t) was used to determine the constant β and the initial adsorption rate. The correlation coefficient values, R^2 for the concentrations of 324mg L^{-1} and 542 mg $L^{-1}$are listed in Table1. The correlation coefficient values for the Elovich kinetic model obtained at the Pb (II) ions concentration of 324 mg L^{-1} and 542 mg L^{-1} were greater than 0.98. This indicates that the adsorption of Pb (II) ions onto TAB is acceptable for this model.

Mechanism of adsorption

The adsorbent material, TAB can be considered to be microporous biopolymer; therefore, pores are large enough to let Pb (II) ions through. The mechanism of Pb (II) ions adsorption on porous adsorbents may involve four steps (i) diffusion of ions to the external surface of bio-adsorbent; (ii) diffusion of ions into the pores of bio-adsorbent; (iii) adsorption of the lead ions on the internal surface of bio-adsorbent. (iv) Interaction between the anionic groups in bioadsorbent (-COOH groups) and the cations in solution. The anionic nature of TAB plays the key role in the adsorption process. The negatively surfaces of the biomass attract the oppositely charged lead cations and brings about stronger complexation.

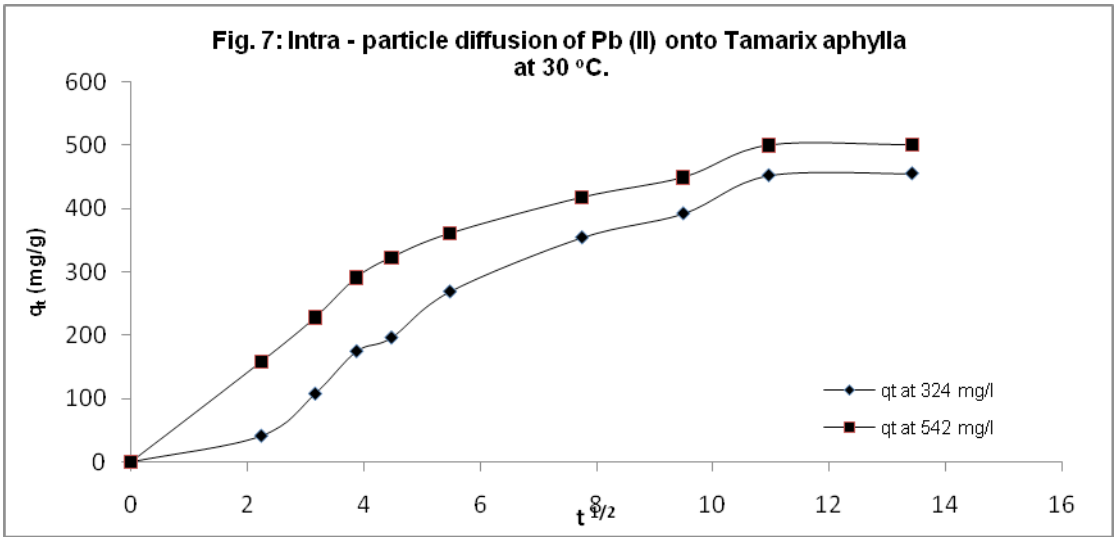
Fig. 7: Intra - particle diffusion of Pb (II) onto Tamarix aphylla at 30 °C.
qt (mg/g)
t 1/2
qt at 324 mg/l
qt at 542 mg/l

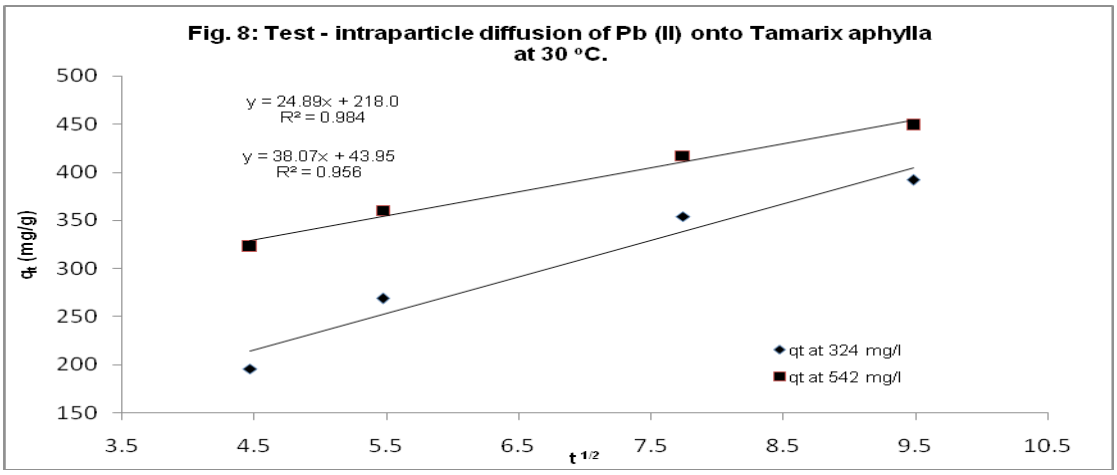
Fig. 8: Test - intraparticle diffusion of Pb (II) onto Tamarix aphylla at 30 °C.
y = 24.89x + 218.0
R² = 0.984
y = 38.07x + 43.95
R² = 0.956
qt (mg/g)
t 1/2
qt at 324 mg/l
qt at 542 mg/l

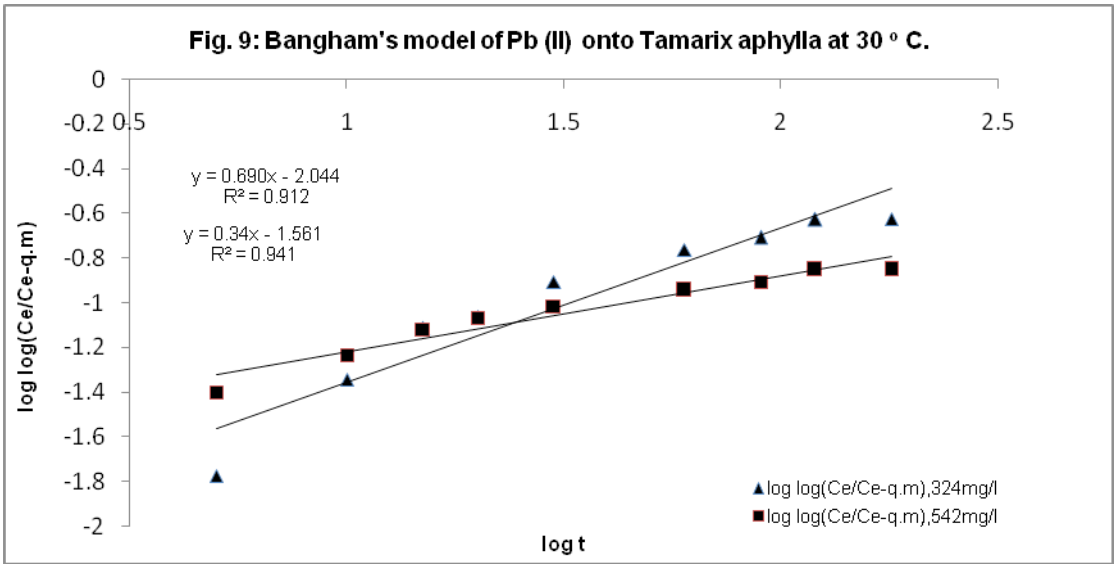
Fig. 9: Bangham's model of Pb (II) onto Tamarix aphylla at 30 ° C.
y = 0.690x - 2.044
R² = 0.912
y = 0.34x - 1.561
R² = 0.941
log log(Ce/Ce-q.m)
log t
log log(Ce/Ce-q.m),324mg/l
log log(Ce/Ce-q.m),542mg/l

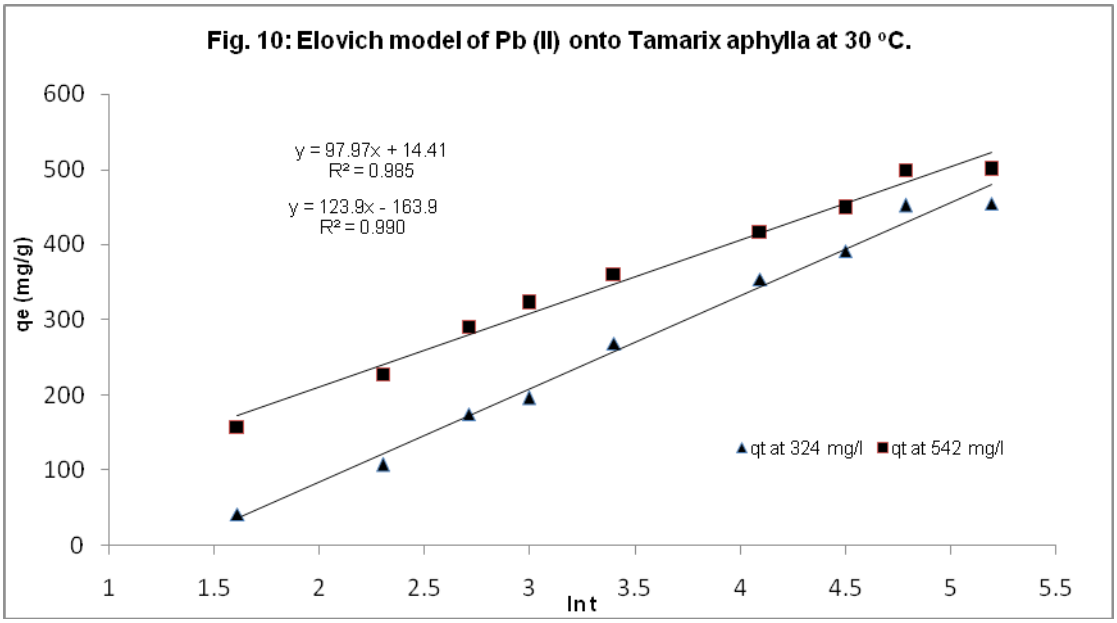

Effect of Adsorbate Concentration

Adsorption Isotherm

Adsorption isotherm, describe how adsorbates interact with adsorbents, is critical in optimizing the use of adsorbents. The amount of adsorbate per unit mass of adsorbent at equilibrium, q_e (mg/g) and the adsorbate equilibrium concentration, C_e (mg L^{-1}) allows plotting the adsorption isotherm, q_e versus C_e (Fig. 11) at 30°C and mathematical models can be used to describe and characterize the adsorption process. The most common isotherms for describing solid–liquid sorption systems are Langmuir, Freundlich, Temkin, Dubinin and Halsey (two parameter isotherms), Redlich–Peterson, Langmuir- Freundlich, Radk-Prausintz, Toth, Sips, Khan and Hill (three parameter isotherms), Weber-van Vliet, Fritz–Schlunder and Baudu (four parameter models) and Fritz–Schlunder (five parameter model). Therefore, in order to investigate the adsorption capacity of Pb (II) ions onto TAB, the experimental data were fitted to these equilibrium models.

Two Parameter Isotherms

Langmuir equation [32] was applied for adsorption equilibrium of Pb (II) ions by TAB. The assumption of this model is based on the maximum adsorption corresponds to a saturated monolayer of adsorbate molecules on the adsorbent surface and the energy of adsorption is constant as well as there is no transmigration of adsorbate in the plane surface. The nonlinear form of Langmuir isotherm is given by the following equation:

$$q_e = \frac{k_L.C_e}{1+a_L.C_e} \quad (15)$$

where a_L is the Langmuir isotherm constant (L/mg), K_L is the Langmuir constant (L/g) and a_L / K_L represents the maximum adsorption capacity, Q_{max}.

The Freundlich model [33] is a special case applied to non-ideal adsorption on heterogeneous surfaces and also to multilayer adsorption, suggesting that binding sites are not equivalent and/or independent. This model is described by Eq. 16 as follows:

$$q_e = K_F.C_e^{1/n} \quad (16)$$

Where q_e is the equilibrium concentration of Pb(II) ions on TABadsorbent (mg/g), C_e the equilibrium concentration of Pb(II) ions(mg L^{-1}) and K_F (mg/g) and n are the Freundlich constants characteristic of the system, indicators of adsorption capacity and adsorption intensity, respectively.

The Temkin isotherm [34] has been used in the following form:

$$q_e = \frac{RT}{b_T}\ln(A_T C_e) \quad (17)$$

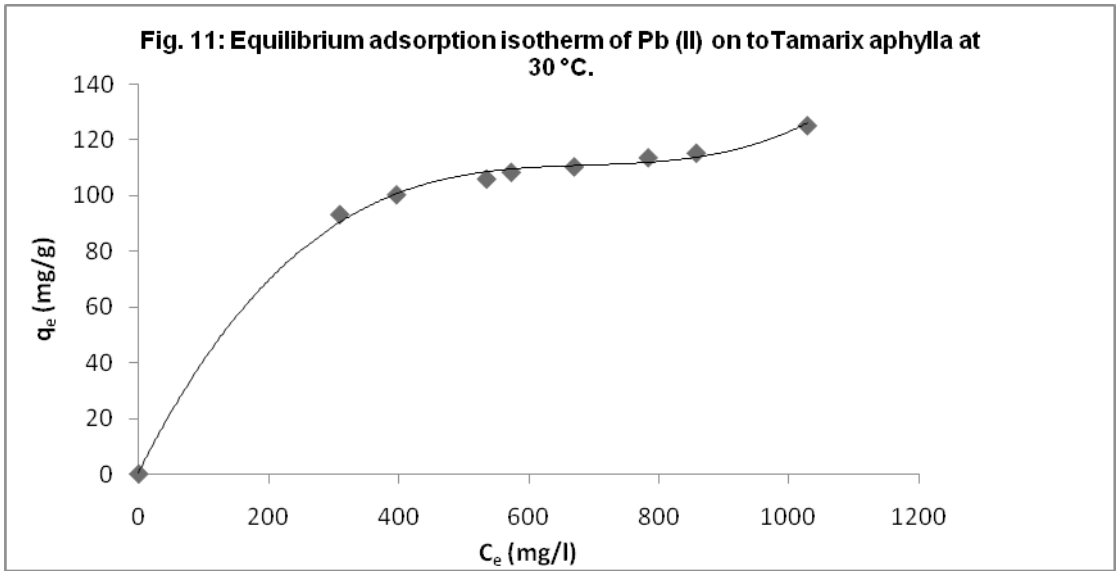

Where R is the universal gas constant (8.31441 $J^{-1}.mol^{-1}.K^{-1}$), T is the absolute temperature (K), A_T is the Temkin isotherm constant (g/mg) and b_T is Temkin constant.

Dubinin-RadushkevichIsotherm [35] is generally expressed as follows:

$$q_e = q_D.\exp(-B_D[RT\ln(1+\frac{1}{C_e})]^2 \quad (18)$$

Dubinin- Radushkevichhave reported that the characteristic sorption curve is related to the porous structure of the sorbent. The constant, B_D is related to the mean free energy of sorption per mole of the adsorbate as it is transferred to the surface of the solid from infinite distance in the solution and this energy can be computed using the following relationship by Hasany and Chaudhary [36] as:

$$E = \frac{1}{\sqrt{2B_D}} \quad (19)$$

The Halsey [37] adsorption isotherm can be given as:

$$q_e = \exp(\frac{\ln k_H - \ln C_e}{n}) \quad (20)$$

Wherek_H and n are the Halsey isotherm constant and exponent, respectively. This equation is suitable for multilayer adsorption and the fitting of the experimental data to this equation attest to the heteroporous nature of the adsorbent.

Three Parameter Isotherms

Redlich–Peterson model is used as a compromise between Langmuir and Freundlich models, which can be written as [38]:

$$q_e = \frac{A.C_e}{1+B.C_e^g} \quad (21)$$

Where q_e is the amount of mercury adsorbed (mg/g) at equilibrium, C_e(mg L^{-1}) is the concentration of adsorbate at equilibrium, A (L/g) and B are the Redlich constants and g is exponent, which lies between 1 and 0.

Toth isotherm model [39] is useful in describing heterogeneous adsorption systems, which satisfying both low and high-end boundary of the concentration [40]. It can be represented by the following equation:

$$q_e = \frac{k_t.C_e}{(a_t+C_e)^{1/t}} \quad (22)$$

where K_T, a_T and t are the Toth isotherm constants.

Sips isotherm [41] is a combined form of Langmuir and Freundlich expressions. Sips model can be represented by the following equation:

where K_S is the Sips model isotherm constant (L/g); a_s the Sips model constant (L/mg) and B_s the Sips model exponent.

$$q_e = \frac{k_s.C_e^{B_s}}{1 + a_s.C_e^{B_s}} \quad (23)$$

a_K are devoted to the model constant and model exponent. Khan isotherm model can be represented by:

where b_k is the Khan model constant, a_k the Khan model exponent and q_K is the maximum uptake (mg/g).

Th n be repres

$$q_e = \frac{q_k.b_K.C_e}{(1 + b_K.C_e)^{a_K}} \quad (24)$$

$$q_e = \frac{\alpha_R.r_R.C_e^{\beta R}}{\alpha_R + r_R.C_e^{\beta R-1}} \quad (25)$$

where, $_{R}$, r_R are Radke-Prausnitz model constants, $_{R}$ is Radke-Prausnitz model exponent.

The Langmuir–Freundlich equation is given by [44]:

$$q_e = \frac{q_{mLF}.(k_{LF}.C_e)^{mLF}}{1 + (k_{LF}.C_e)^{mLF}} \quad (26)$$

where, q_{mLF} is the Langmuir-Freundlich maximum adsorption capacity (mg/g), k_{LF} is the equilibrium constant for a heterogeneous solid and M_{LF} is the heterogeneity parameter lies between 0 and 1.

Hill model [45], assumes that adsorption process as a cooperative phenomenon, with the ligand binding ability at one site on the macromolecule, may influence the different binding sites on the same macromolecule. It is described by the following equation:

$$q_e = \frac{q_{s_H}.C_e^{n_H}}{k_D + C_e^{n_H}} \quad (27)$$

Where k_D, n_H and s_H are constants for Hill model.

Four parameter isotherms

Baudo isotherm [46] can be written in the following form:

$$q_e = \frac{qmo.bo.C_e^{(1+x+y)}}{1 + bo} \quad (28)$$

Where q_e is the adsorbed amount at equilibrium (mg/g), C_e is the equilibrium concentration of adsorbate (mg L^{-1}), q_{mo} is the Baudo maximum adsorption capacity (mg/g), b_o is the equilibrium constant, and x and y are the Baudo parameters.

Fritz-Schlunder isotherm

Another four-parameter equation of Langmuir–Freundlich type was developed empirically by Fritz and Schlunder [47]. It is expressed by the equation:

$$q_e = \frac{A.C_e^{\alpha}}{1 + B.C_e^{\beta}} \text{ with } \_, \_ \leq 1 \quad (29)$$

Where q_e is the adsorbed amount at equilibrium (mg/ g), C_e is the equilibrium concentration of adsorbate (mg L^{-1}), *A* and *B* are the Fritz–Schlunder parameters, and α and ß are the Fritz–Schlunder equation exponents. At high liquid-phase concentrations of the adsorbate, the last equation reduces to the Freundlich equation.

Five parameter isotherm

Fritz-Schlunder isotherm

Fritz and Schlunder [47] have proposed a five-parameter empirical expression which can represent a broad field of equilibrium data as:

$$q_e = \frac{q_{mFS}.k_1.C_e^{m_1}}{1 + k_2.C_e^{m_2}} \quad (30)$$

Where q_e is the adsorbed amount at equilibrium (mg/ g), C_e is the equilibrium concentration of adsorbate (mg L^{-1}), q_{mFS} is the Fritz-Schlunder maximum adsorption capacity(mg/g) and K_1, k_2, m_1 and m_2 are Fritz-Schlunder parameters.

The comparison of the adsorption capacity of various adsorbents reported in the literature for the removal of Pb (II) ions is shown in Table 2 [48-54]. It was found from this table that the TAB had a good affinity for removal of lead than other adsorbents.

The comparison between the experimental data and the data obtained from two, three, four and five parameter models (Fig. 12-15) as well as the constants and error analysis of two, three, four and five parameter models are given in Tables 3 -6.

Error Analysis and Non-linear Regression Method

In nonlinear regression method, the validity of widely used isotherm models to the experimental data was examined by trial- and-error using the

TABLE 2. Comparison of adsorption capacity of Pb(II) ions with different adsorbents

Adsorbents	Adsorption capacity (mg/g)	References
Cotton waste	44.67	1
Bog iron ores	97.0	2
Oedogonium species	145	3
Rice husk	12.61	4
Activated charcoals (bamboo)	53.76	5
Almond	8.08	6
Banana peels	72.79	7
Tamarixaphylla	125	This study

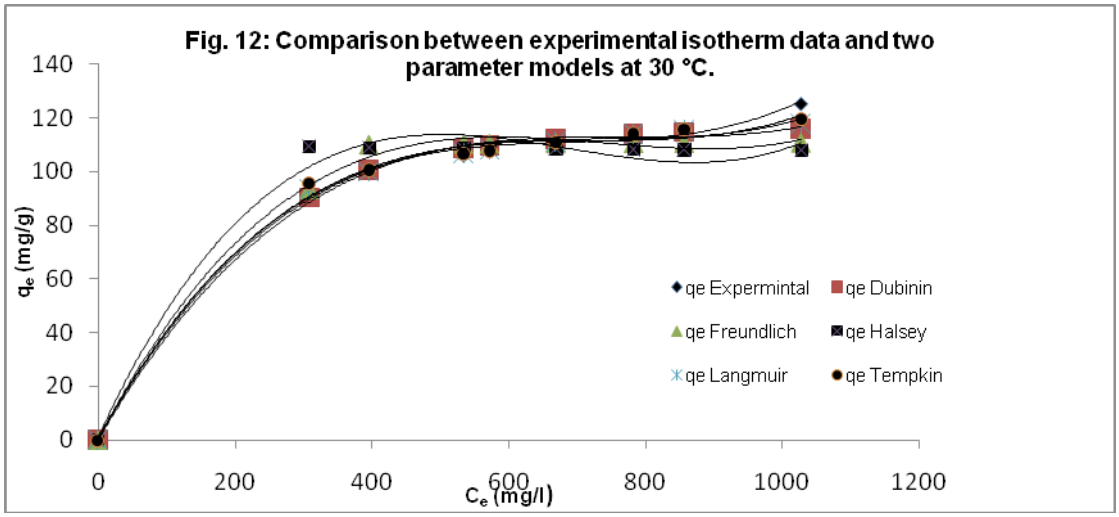

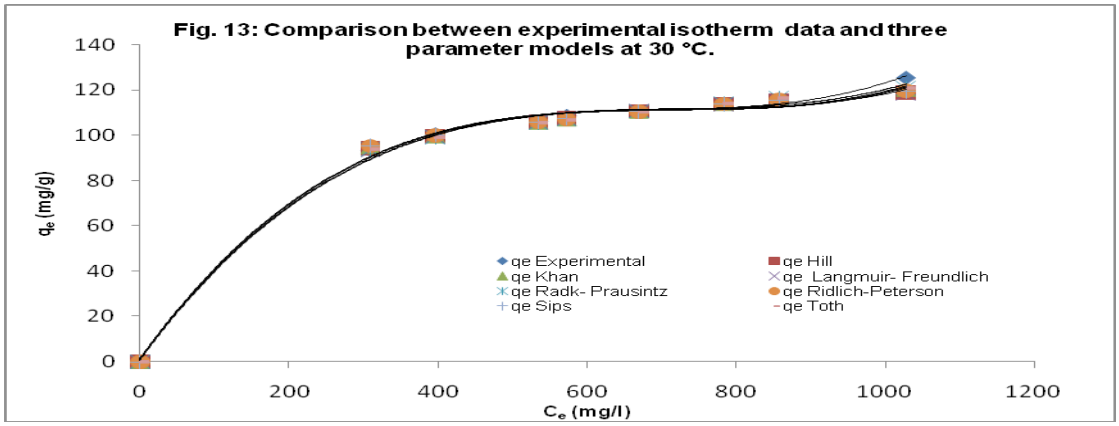

solver add-in with Microsoft Excel. The R^2 value is used to minimize the error distribution between the experimental equilibrium data and the predicted isotherms.

The fitting presentation of two, three, four and five parameter models are presented in Fig. (12-15) as well as the constants and error analysis of two and three parameter models are given in Tables 4-7.

Among two, three, four and five parameter

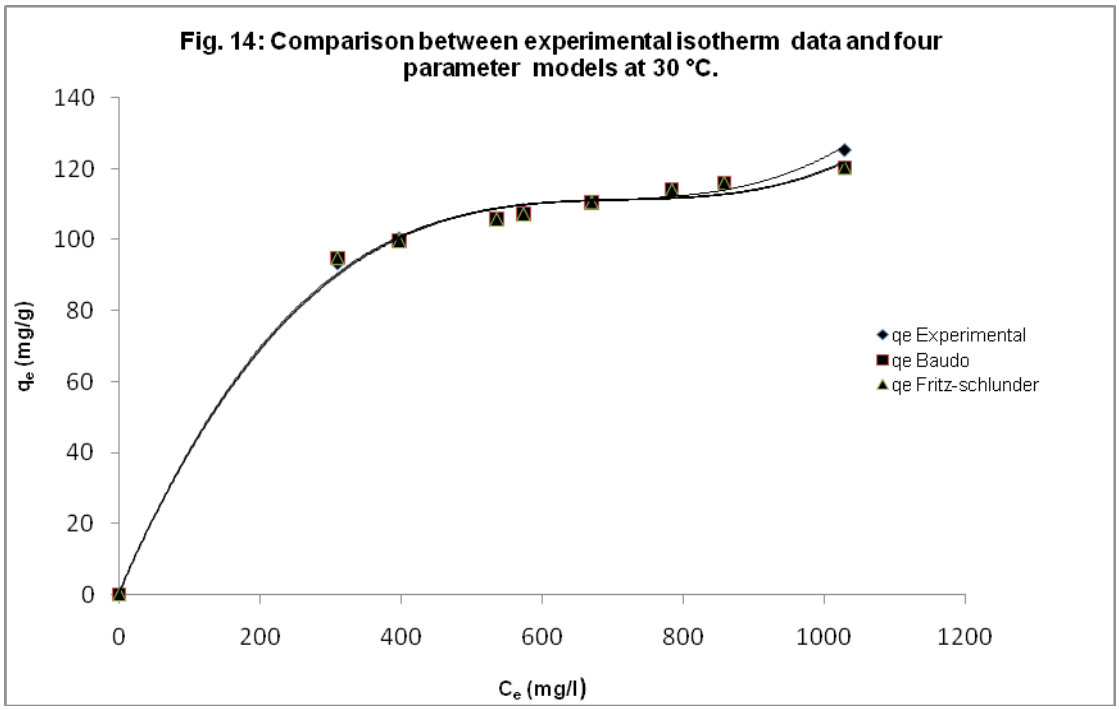

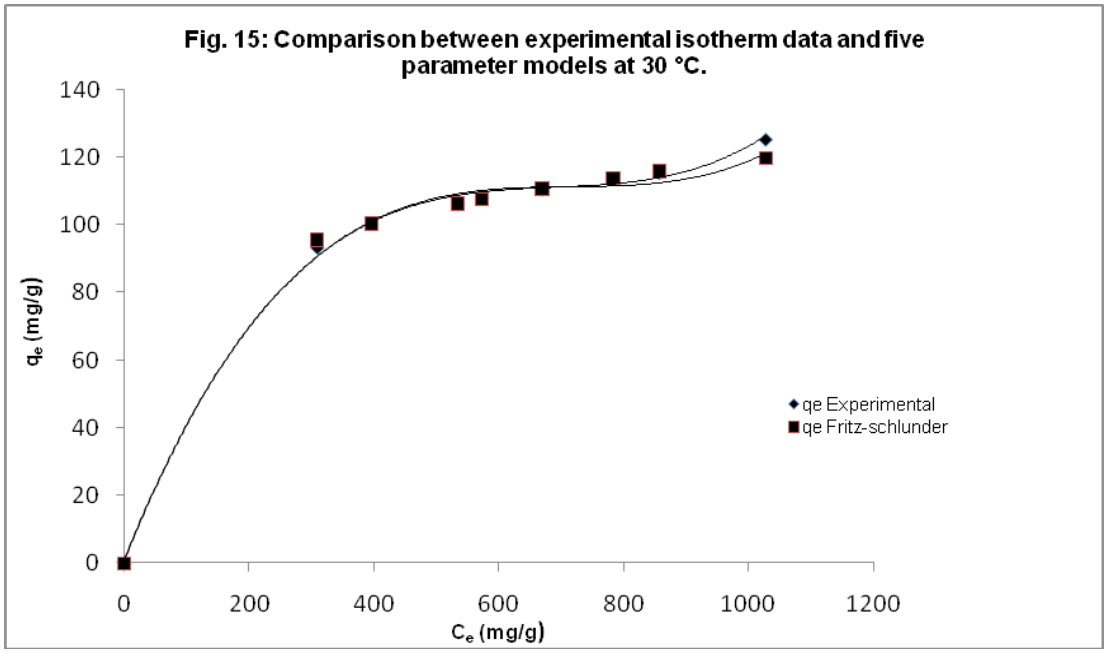

TABLE 3. Constants and error analysis of two parameter models for adsorption of Pb (II) onto TAM at 30 °C

Isotherm Model	Parameter	Value	Error Analysis	Value
Langmuir	a_L	1.000951195	ARE	0.075758395
			APE %	0.9469799939
	k_L	0.00744791	EABS	9.164793121
			MPSD	0.927498356
	R^2	0.9966		
Freundlich	1/n	0.227575233	ARE	0.329443102
			APE %	4.118038773
	K_F	25.3150899	EABS	37.33343094
			MPSD	0.9471997715
	R^2	0.996		
Tempkin	A_T	118.5116757	ARE	0.153246268
			APE %	0.153246268
	b_T	42.035402173	EABS	17.53049319
			MPSD	0.935331558
	R^2	0.9989		
Radushkevic Dubininh	q_D	118.5116757	ARE	0.153246268
			APE %	1.915578349
	B_D	42.035402173	EABS	17.53049319
			MPSD	0.935331558
	R^2	0.9989		
Halsey	K_H	27.34163349	ARE	0.09759607
			APE %	1.219950869
	n	-4.658446352	EABS	11.02817686
			MPSD	0.92292599
	R^2	0.9949		

TABLE 4. Constants and error analysis of three parameter models for adsorption of Pb(II) onto TAM at 30 °C

Isotherm Model	Parameter	Value	Error Analysis	Value
Redlich-Peterson	A	18.72786112	ARE	0.09377391
			APE %	1.172173873
	B	0.538773491	EABS	10.56033499
			MPSD	0.927892413
	g	0.820870841		
	R^2	0.9966		
Toth	k_t	34.03614	ARE	0.097299121
			APE %	1.216239014
	a_t	0.099071892	EABS	10.86179667
			MPSD	0.929013861
	1/t	0.818816538		
	R^2	0.996		
Sips	K_s	28.92339167	ARE	0.093193116
			APE %	1.164913948
	a_s	0.078628279	EABS	10.51013395
			MPSD	0.92835949
	B	0.261187618		
	R^2	0.9943		
Khan	q_k	17.77438307	ARE	0.097229509
			APE %	1.215368861
	a_k	0.788696068	EABS	10.97983007
			MPSD	0.924635814
	b_k	8.51802902		
	R^2	0.9943		
Hill	q_{SH}	164.799183	ARE	0.087695156
			APE %	1.096189445
	K_D	15.65047066	EABS	10.09566861
			MPSD	0.928591569
	n_H	0.534170146		
	R^2	0.9951		
Langmuir- Freundlich	q_{mLF}	143.3484032	ARE	0.082409362
			APE %	1.030117027
	K_{LF}	0.007796297	EABS	9.675424086
			MPSD	0.928878314
	m_{LF}	0.753518481		
	R^2	0.9957		
Radke-Prausnitz	_R	154.856542	ARE	0.094487849
			APE %	1.181098115
	rR	33.16282288	EABS	10.60827109
			MPSD	0.928124744
	_R	0.185162467		
	R^2	0.9942		

TABLE 5. Constants and error analysis of four parameter models for adsorption of Pb (II) onto TAMat 30 °C

Isotherm Model	Parameter	Value	Error Analysis	Value
Baudo	Qm	34.10876755	ARE	0.095916745
			APE%	1.198959317
	b0	7.977238838	EABS	7.977238838
			MPSD	0.927831759
	x	-2.329844291		
	y	1.528671215		
	R2	0.9945		
Fritz-Schlunder	A	5.091624734	ARE	0.096402932
			APE%	1.205036653
	α	1.296219342	EABS	10.92977435
			MPSD	0.926928828
	B	0.176106953		
	β	1.062271408		
	R^2	0.995		

models, the highest R^2 value and lowest ARE, APE %, EABS, and MPSD indicated that Langmuir (two parameter isotherm) is the better fit than the rest of isotherm models.

Conclusions

TAB has been utilized as adsorbent material for the removal of Pb(II) ions from contaminated water. The ability of TAB to adsorb Pb(II) ions was investigated by using batch adsorption procedure. The data of the adsorption isotherm was tested by two, three, four and five parameter models by using non-linear regression technique. The best fitting model was first evaluated using four different error functions. The examination of all these error estimation methods showed that the Langmuir model provides the best fit for experimental data than other isotherms. The kinetics of adsorption of Pb (II) ions have been discussed using five kinetic models, i.e., the pseudo-first-order, the pseudo-second-order, Elovich, intraparticle diffusion and Bangham models. The adsorption of Pb(II) ions onto TAB could be well described by the pseudo-second-order kinetic model.

References

1. Ucar, S, Erdem, M, Tay, and T, Karagoz, S, Removal of lead (II) and nickel (II) ions from aqueous solution using activated carbon prepared from rapeseed oil cake by Na_2CO_3 activation, *Clean. Technol. Environ. Policy*, **17**, 747–756 (2015).

2. Pei-Sin Keng, Yung-Tse Hung, Siew-Ling Lee, Siew-Teng Ong and Sie-Tiong Ha, Removal of hazardous heavy metals from aqueous environment by low-cost adsorption materials, *Environ Chem. Lett*, **12,** 15–25 (2014).

3. Ajmal, M. Rao, R.A. Anwar, S. Ahmad, J. and Ahmad, R. Adsorption studies on rice husk: removal and recovery of Cd (II) from wastewater, *Bioresour Technol*, **86**, 147-9 (2003).

4. Brown, P.A. Gill, S.A. Allen, S.J. Metal removal from wastewater using peat. *Water Res*. **34**, 3907–3916 (2000).

5. S.K. Chandra, C.T. Kamala, N.S. Chary, Y. Anjaneyulu, Removal of heavy metals using a plant biomass with reference to environmental control. Int. *J. Miner. Proc*. **68** 37–45 (2003).

6. M.M. Nassar and M.S. El-Geundi, Comparative cost of color removal from textile effluents using natural adsorbents*, J. Chem. Technol. Biotechnol*. **50** 257-264(1991).

7. G. McKay, Adsorption of dyestuff from aqueous solution with activated carbon: I. Equilibrium and batch contact time studies, *J. Chem. Technol. Biotechnol*. **32,** 759-772 (1982).

8. A. Hashem, A. Akasha, A. Ghith and D. A. Hussein,Adsorbent based on agricultural wastes for heavy metal and dye removal: a review, *Ener. Educ. Sci. Technol*. **19,** 69-8 (2007).

9. M, Anari-Anaraki, A, Nezamzadeh-Ejhieh, Modification of an Iranian clinoptilolitenano-particles by hexadecyltrimethyl ammonium cationic surfactant and dithizone for removal of Pb(II) ions from aqueous solution, *Journal.*

of Colloid and Interface. Science **440,** 272–281 (2015).

10. P, Castaldi, M, Silvetti, G,Garau, D, Demurtas, S,Deiana,Copper(II) and lead(II) removal from aqueous solution by water treatment residues, *Journal of Hazardous Materials* **283,** 140–147 (2015).

11. R,Karthik, S, Meenakshi, Removal of Pb(II) ions and Cd (II) ions from aqueous solution usingpolyaniline grafted chitosan, *Chemical Engineering Journal* **263,** 168–177 (2015).

12. R, Chen, Y, Zhang, L, Shen, X, Wang, J, Chen, A, Ma,W, Jiang, Lead(II) and methylene blue removal using a fully biodegradablehydrogel based on starch immobilized humic acid, *Chemical Engineering Journal* **268,** 348–355 (2015).

13. S, Indah Raya, M,Zakir, The Adsorption of Pb(II) ions on activated carbon from rice husk, Irradiated by ultrasonic waves:Kinetic and thermodynamics studies, *Journal of Natural Sciences Research*, **4,**18-24 (2014).

14. M, Kafia, S, Surchi, Agricultural wastes as low cost adsorbents for Pb removal: Kinetics, equilibrium and thermodynamics, *International Journal of Chemistry*, **3,**103-112 (2011).

15. S. C. Tsai, K. W. Juang, Comparison of linear and non-linear forms of isotherm models for strontium sorption on a sodium bentonite, *J. Radio Ana NucChem*. **243,** 741–746 (2000).

16. Z. Aksu, Determination of the equilibrium, kinetic and thermodynamic parameters of the batch biosorption of nickel (II) ions onto Chlorella vulgaris, *Process Biochemistry* **38,** 89–99 (2002).

17. P. X.Sheng, Y. P. Ting, J. P., Chen, Hong, Sorption of lead, copper, cadmium, zinc, and nickel by marine algal Biomass: Characterization of biosorptivecapacity and investigation of mechanisms, *Journal of Colloid and Interface Science*, **275,** 131-141 (2004).

18. V. Padmavathy, P. Vasudevanand, S. C, Dhingra, Bio- sorption of nickel(II) ions on baker's yeast, Process Biochemistry, **38**, 1389-1395 (2004).

19. S. V, Dimitrova, Metalsorption on blast furnace slag, *Water Research*, **30,** 228-232 (1996).

20. A. Hashem, R.A. Akasha, D.M. Hussein and A. Ghith, Synthesis, characterization and application of cellulose maleate based on sawdust for Pb(II) ions removal from aqueous solution, *Energy Education Science and Technology*, **18**, 67-83 (1996).

21. A.Hashem, A.Abou-Okeil, A. El-Shafie, M.El-Sakhawy, Grafting of high _-cellulose pulp extracted from sunflower stalks for removal of Hg (II) from aqueous solution, *Polymer-Plastics Techno Eng*. **45,** 135–141 (2006).

22. H.C. Trivedi, V. M. Patel, R. D. Patelm Adsorption of cellulose triacetate on calcium silicate. *EurPolym J*. **9,** 525–531 (1973).

23. Y. S. Ho, G. McKeay, The kinetics of sorption of divalent metal ions onto sphagnum moss peat. *Water Res* **34,** 735-742 (2000).

24. W. J. Weber, J. C. Morris, Advances in water pollution research. Proc. 1st Int. Conf. on *Water Pollution Res*. **2,** 231-266 (2000).

25. H. K. Boparai, M. Joseph, De. M. O'Carroll, Kinetics and thermodynamics of cadmium ion removal by adsorption onto nanozerovalent iron particles, *J. Hazard. Mater*. **186,** 458–465 (2011).

26. E.I. Unuabonah, K.O. Adebowale, B.I. Olu-Owolabi, Kinetic and thermodynamic studies of the adsorption of lead (II) ions onto phosphate-modified kaolinite clay, *J. Hazard. Mater*. **144,** 386–395 (2011).

27. F.C. Wu, R.L. Tseng, R.S. Juang, Initial behavior of intraparticle diffusion model used in the description of adsorption kinetics, *Chem. Eng. J*. **153**, 1–8 (2011)

28. V. J. P. Poots, G. McKay, J. Healy, Removal of basic dye from effluent using wood as an adsorbent. *J. Water. Pollut. Control Federation* **50,** 926–935 (1978).

29. K. Nagarethinam, M.S. Mariappan, Kinetics and mechanism of removal of methylene blue by adsorption on various carbons-a comparative study. *Dyes Pigm* **51**, 25-40 (1978).

30. E, Tutem, R,Apak, C.F. Unal, Adsorptive removal of chlorophenols from water by bituminous shale. *Water Res* **32**, 2315–2324 (1978).

31. S. H. Chien, W. R. Clayton, Application of Elovich equation to the kinetics of phosphate release and sorption in soils. *Soil Sci. Soc. Am* J. **44**, (1978)

32. I. Langmuir, The constitution and fundamental properties of solids and liquids, *J. Am. Chem. Soc*. **38,** 2221-2295 (1916).

33. H. Freundlish, Over the adsorption in solution, *J. Phys. Chem*., **57,** 385-470 (1906).

34. M.J. Tempkin, V. Pyzhev, Kinetics of ammonia

synthesis on promoted iron catalysts*, Acta, Physiochim*, URSS, **12**, 217-222 (1906).

35. M. M. Dubinin, Modern state of the theory of volume filling of micropore adsorbents duringadsorption of gases and steams on carbon adsorbents, *Zhurnal. Fizicheskoi. Khimii* **39,** 1305–1317(1965).

36. S.M. Hasany, and M. H. Chaudhary, Sorption potential of Hare River sand for the Removal of antimony from acidic aqueous solution, *Appl. Rad. Isot*. **47**,467–471 (1996).

37. G. Halsey, Physical Adsorption on non-uniform surfaces. *J. Chem. Phys*. **16,** 931-937 (1948).

38. O.Redlich, D. Peterson, A useful adsorption isotherm, *J. Phys. Chem*. **63,** 1024–1026 (1959).

39. J. Toth, State equations of the solid gas interface layer, *Acta Chem. Acad. Hung*. **69,** 311–317 (1971).

40. K. Vijayaraghavan, T.V.N. Padmesh, K. Palanivelu, M. Velan, Biosorption of nickel (II) ions onto Sargassumwightii: application of two-parameter and three parameter isotherm models, *J. Hazard. Mater*. **B133**, 304–308 (2006).

41. R. Sips, Combined form of Langmuir and Freundlich equations, *J. Chem. Phys*. **16,** 490–495 (1948).

42. A.R. Khan, R. Ataullah, A. Al-Haddad, Equilibrium adsorption studies of some aromatic pollutants from dilute aqueous solutions on activated carbon at different temperatures, *J. Colloid Interface Sci*. **194,** 154–165 (1997).

43. C.J. Radke, J.M. Prausnitz, Adsorption of organic solutions from dilute aqueous solution on activated carbon, *Ind. Eng. Chem. Fund*. **11,** 445–451 (1972).

44. R. Sips, On the structure of a catalyst surface, *J. Chem. Phys.* **16**, 490–495 (1948).

45. K. Y. Foo and B. H. Hameed, Insights into the modeling of adsorption isotherm systems, *Chem. Eng. J*., vol. **156**, pp. 2-10, (2010).

46. M. Baudu, Etude des interactions solute-fibres de charbonactif. Application et regeneration, *Ph. D. Thesis,* Universite de Rennes. *I* (1990).

47. W. Fritz, E.U. Schlunder, Simultaneous adsorption equilibria of organic solutes in dilute aqueous solution on activated carbon, *Chem. Eng. Sci*. **29** 1279–1282 (1974).

48. M. Riaza, R. Nadeema, M.A. Hanifa, T.M.Ansaric and K. Rehmana, Pb(II) biosorption from hazardous aqueous streams using Gossypiumhirsutum (Cotton) waste biomass, *Journal of Hazardous Materials*, **161**, 88–94 (2009).

49. G. Rzepa, T. Bajda and T. Ratajczak Utilization of bog iron ores as sorbents of heavy metals, *Journal of Hazardous Materials*, **162,** 1007–1013 (2009).

50. V.K. Gupta, A. Rastogi, Biosorption of lead (II) from aqueous solutions by non-living algal biomass Oedogonium sp. and Nostoc sp.: a comparative study, *Colloids Surf. B: Biointerfaces*, **64,**170–178 (2008).

51. Q. Feng, Q. Lin, F. Gong, S. Sugita and M. Shoya, Adsorption of lead and mercury by rice husk ash, *Journal Of Colloid And Interface Science*, **278,** 1–8 (2004).

52. H. Lalhruaitluanga, K. Jayaram, M.N.V. Prasad, K.K. Kumar, Pb(II) adsorption from aqueous solutions by raw and activated charcoals of Melocannabaccifera Roxburgh (bamboo): a comparative study. *J. Hazard. Mater*. **175,** 311–318 (2010).

53. E. Pehlivan, T. Altun, S. Cetin, M.I. Bhanger, Pb (II) sorption by waste biomass of hazelnut and almond shell. *J. Hazard. Mater.* **167**, 1203–1208 (2009).

54. J. Anwar, S. Umer, Waheed-uz-Zaman, M. Salman, A. Dar, S. Anwar, Removal of Pb (II) and Cd (II) from water by adsorption on peels of banana. *Bioresour.Technol* **101**,1752–1755 (2010).

(*Received 12/9/2017*;
accepted 1/2/2018)

نبات التاماريكس أفيلا كمادة ادمصاص فعالة لإزالة أيونات الرصاص من المحاليل المائيةحركية الادمصاص ومدى موافقة نتائج الادمصاص على نماذج الإيزوثرم المختلفة

مجدي دياب مدبولي[١] و علاء الأنور[٢]
[١] المركز القومي للبحوث الاجتماعية والجنائية ، القاهرة، مصر
[٢]مصلحة الطب الشرعي، وزارة العدل ، معمل أسيوط

في هذه الدراسة تم استخدام التاماريكس أفيلا كمادة مدمصة رخيصة الثمن لإزالة أيونات الرصاص من المحاليل المائية.

وقد تميزت الدراسة باستخدام طيف الأشعة تحت الحمراء وميكروسكوب المسح الألكتروني لتأكيد عملية الادمصاص. وقد وضحت النتائج قدرة النبات على ادمصاص أيونات الرصاص بطريقة الادمصاص الساكنة . وتمت دراسة العوامل المختلفة التى تؤثر على عملية الادمصاص ومنها تأثير الرقم الهيدروجيني للمحلول، تركيز المادة الماصة، تركيز المادة المدمصة والوقت. وتم في هذه الدراسة مطابقة النتائج بخمسة أنواع من نماذج الأيثوثيرم المختلفة عند درجة حرارة 30 درجة مئوية باستخدام معامل الارتباط. وكذلك تضمنت الدراسة الحركية الكيميائية لعملية الادمصاص باستخدام نماذج مختلفة من تفاعل الرتبة الأولى الكاذبة والرتبة الثانية الكاذبة، إلوفيتش، وتغلغل الجسيمات في المسافات البينية ونموذج بانجام على البيانات التجريبية للتنبؤ بميكانيكية الادمصاص. وقد بينت النتائج الحركية أن تفاعل الادمصاص يتوافق مع الرتبة الثانية الكاذبة أكثر من النماذج الآخرى. كما أظهرت النتائج أيضاً أن نموذج لانجمير هو أقرب نماذج الأيزوثيرم المستخدمة مع النتائج التجريبية المتحصل عليها مما يؤكد أن النبات يمكن استخدامه كمادة فعالة ورخيصة الثمن لإزالة أيونات الرصاص من المحاليل المائية.